

## Article

# Lithofacies and Sediment Sequences of a Microtidal, Wave-Dominated Tropical Estuary in Somone Lagoon (Senegal, West Africa)

Cheikh Ibrahima Youm <sup>1</sup>, Adama Gueye <sup>1</sup>, Elena García-Villalba <sup>2</sup>, Mbemba F. Doumbouya <sup>1</sup>, Ibrahima-Sory Sow <sup>3</sup>, Elhadji Sow <sup>1</sup> and Juan A. Morales <sup>2,\*</sup> 

<sup>1</sup> Faculty Sciences and Techniques, University Cheikh Anta Diop, Dakar-Fann S-5005, Senegal; cheikhibrahima.youm@ucad.edu.sn (C.I.Y.); gueyeucad@gmail.com (A.G.); mbemba9519@gmail.com (M.F.D.); elhadji.sow@ucad.edu.sn (E.S.)

<sup>2</sup> Scientific and Technological Center of Huelva, Earth Sciences Department, University of Huelva, E-21007 Huelva, Spain; elena.garcia869@alu.uhu.es

<sup>3</sup> Faculty of Letters and Human Sciences (FLSH), University Cheikh Anta Diop, Dakar-Fann S-5005, Senegal; sorysown@gmail.com

\* Correspondence: jmorales@uhu.es

**Abstract:** Estuary sedimentary sequences have been the focus of several papers in the last decades; however, the majority these papers were centered in mesotidal and macrotidal estuaries of the middle latitudes. This present paper studies, from a sedimentological point of view, the infilling of a microtidal, wave-dominated tropical estuary, where wide tidal flats, mangroves and sabkhas are developed. Somone Lagoon is a Senegalese protected environment, very rich from an ecological point of view and with a definitive touristic vocation. For this work, 14 piston cores were studied. Additionally, the grain size, calcium carbonate and organic matter contents of 61 sediment samples vertically distributed in these cores were analyzed. The distribution of facies and the vertical sequences of sediments show the influence of the tropical seasonal fluctuations of fluvial sediment supply and evaporation processes. A high degree of bioturbation and an elevated organic content can be interpreted as the result of a high capacity of retention of the organic material into the estuary influenced by the weak tidal currents typical of a microtidal regime. These processes, acting since the last Holocene invasion of sea level, caused an advanced state of infilling of this estuarine system where both flood tidal deltas and bay head deltas prograde above the fine facies of the central domain of the estuary.

**Keywords:** sedimentology; estuarine infilling; tidal flats; mangroves; sabkhas; Senegal



**Citation:** Youm, C.I.; Gueye, A.; García-Villalba, E.; Doumbouya, M.F.; Sow, I.-S.; Sow, E.; Morales, J.A. Lithofacies and Sediment Sequences of a Microtidal, Wave-Dominated Tropical Estuary in Somone Lagoon (Senegal, West Africa). *Coasts* **2024**, *4*, 306–322. <https://doi.org/10.3390/coasts4020016>

Received: 2 February 2024

Revised: 22 March 2024

Accepted: 1 April 2024

Published: 5 April 2024



**Copyright:** © 2024 by the authors. Licensee MDPI, Basel, Switzerland. This article is an open access article distributed under the terms and conditions of the Creative Commons Attribution (CC BY) license (<https://creativecommons.org/licenses/by/4.0/>).

## 1. Introduction

Estuaries are semi-enclosed bodies of coastal waters that connect a fluvial system to the open sea and where fresh water coming from river drainage is diluted with the sea water [1]. In general terms, it is a type of river mouth in which the main sedimentation processes occur in the interior of a coastal valley in relation with the development of fresh and saltwater mixing [2].

The genesis of estuarine valleys has been attributed to relative sea level rises [3]. After that, the beginning of the infilling of present estuaries is the Flandrian post-Würm transgression which invaded the pre-existing fluvial valleys entering the marine agents and transforming them into coastal embayments. Since this starting point, the general trend of all the estuaries during the Holocene is the infilling of these valleys with sediment from the following three sources: fluvial, marine and autochthonous [4]. The distribution of sediments in an estuarine system corresponds, in the short term, to three fundamental agents: river, tides and waves. The space distribution of these three agents controls the

existence of the following three estuarine domains [5]: a marine domain marked by the balance between waves and tides, a central estuary dominated by tides and a fluvial domain controlled by the balance between fluvial and tidal currents. In the long term, there is a control exerted by the relationships between relative sea level movements and sedimentary input. Climate also exerts a secondary influence in the short and long term, because it controls the intensity of physical, chemical and biological processes, the sedimentary input and the sea level [2]. The combination of all these factors will directly control the facies sequences in each domain of the estuary and the evolutionary trends of the system.

At least six different classifications of estuaries have been defined using a variety of criteria as the model of mixing waters [5], the genetic process [6], the model of propagation of the tide [7], the tidal range [8] or the estuarine physiography [9]. Nevertheless, from a geological point of view, the most adequate criterion to classify estuaries is the dynamic balance between processes [10]. Using this criterium, the following two types of estuaries can be distinguished according to the dominant agent: tide-dominated and wave-dominated. Each one of these types of estuaries present a characteristic morphology, a specific facies distribution and an evolutionary trend.

The aim of this paper is to study a wave-dominated estuary located in an African microtidal tropical coast, in Somone Lagoon in Senegal, West Africa. Drawing on sedimentological data and facies interpretation, this work has regional importance, since papers studying African estuaries are scarce [11]. In general terms, wave-dominated estuaries are well studied (e.g., [12–14]), but there are few works that analyze wave-dominated estuaries in microtidal tropical contexts that also present a mixture of detrital and carbonate elements and a notable influence of evaporitic processes. This estuary, by its combination of characteristics, is a potentially important natural laboratory to analyze the impacts of competing processes on estuary evolution, including generation and preservation of facies sequences. For that, this study also has a clear thematic interest.

### 1.1. Regional Setting

Somone lagoon is a natural reserve of community interest, created in 1999 by a regional request supported by the National Parks Department of the Senegal Republic. The estuarine system has an area of 7 km<sup>2</sup> which is located at the mouth of the Somone River in the northern Small Coast (Petite-Côte), 40 km to the southeast of the city of Dakar and 14 km to the north of the city of Mbour (Figure 1). This is a small system formed by the marine inundation of a fluvial valley. The valley was incised in the Campanian–Maastrichtian (Upper Cretaceous) unconsolidated sandstones and clays. These materials were deposited in the Dias Horst [15] during the lowstand period associated with the Würm glacial maximum [16]. Subsequently, this depression was flooded by the sea during the Nouakchottian stage of the Flandrian transgression, which occurred between 5500 and 4100 years B.P. [17]. Since the marine invasion of the valley, the system has sustained limited accommodation due to a high sediment supply. At the same time, the growth of the spits and flood-tidal deltas closed the inner domains, inducing a deficient tidal drainage. As a consequence of this lack of flushing, previous studies indicate that the system is ecologically eutrophized and degraded [18].

### 1.2. Environment Physiography

The present physiography of Somone Lagoon and all local geographic names are shown in Figure 1. In the marine domain, a 1.8 km long spit (Cape Guereo) restricts the inner zone of the estuary to its wave action. The berm lines indicate a sense of growing towards the south as an effect of an N–S littoral drift. The town of Guereo is located at the contact of this spit with the continent. As a second sandy form closes the estuary, a short 300 m counterspit grew from the south. This counterspit originated from waves refracted by sandy, estuary mouth shoals.

The town of Somone is located at the south of the start point of this counterspit. In the outer front of the inlet, a small wave-dominated ebb-tidal delta is developed. The

aforementioned sandy shoals correspond with the frontal lobe and swash bars of this delta. On the back area located at the entrance of the estuarine system, two flood-tidal deltas are developed (Figure 2A). The first one is protected by the counterspit. It is currently less active, since it is not directly connected with the inlet and corresponds to an older growth stage of the counterspit. The second one is the most recent of them. It was developed at the end of the present inlet and is dynamically active. In the central domain, a wide tidal system has developed. From a hydrological point of view, two areas were distinguished, the central basin and the Guereo Basin. The central basin (Figure 2B) is located at the center of the estuary, connecting fluvial and marine domains. The Guereo Basin (Figure 2C) is a marginal lagoon located in the back area of the Cape Guereo spit. Both basins are now connected by some tidal channels but constituted just one single basin in previous infilling stages of the estuary. In both areas, tidal channels and creeks separate various islands constituted by tidal flats and mangroves. In the fluvial domain, a prograding bay head delta is developed. Presently, the most superficially extensive sub-environments associated to this inner delta are evaporitic coastal sabkhas.

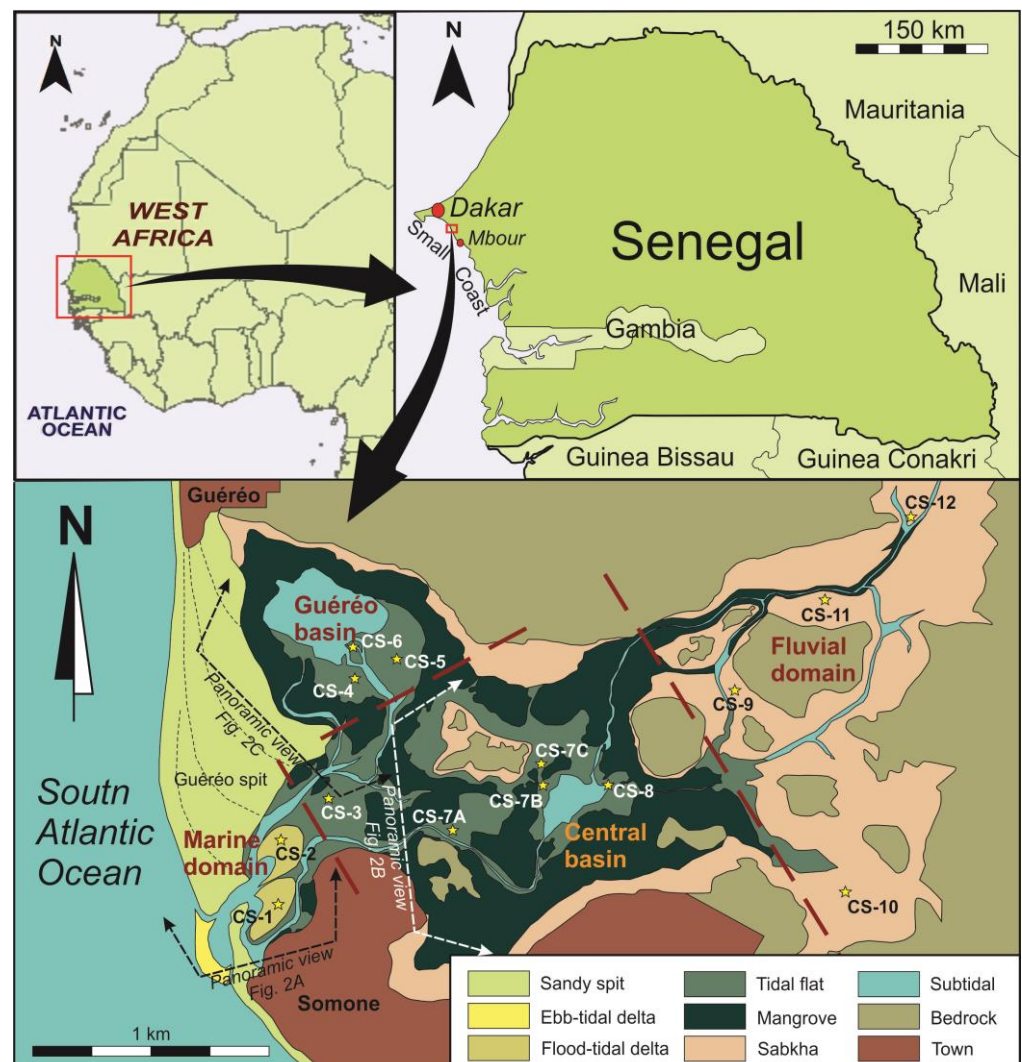


**Figure 1.** Location of the study area and sub-environment map indicating the domains of the estuary, the geographic names and the locations of the cores (stars). The positions of panoramic views of Figure 2 are also indicated.

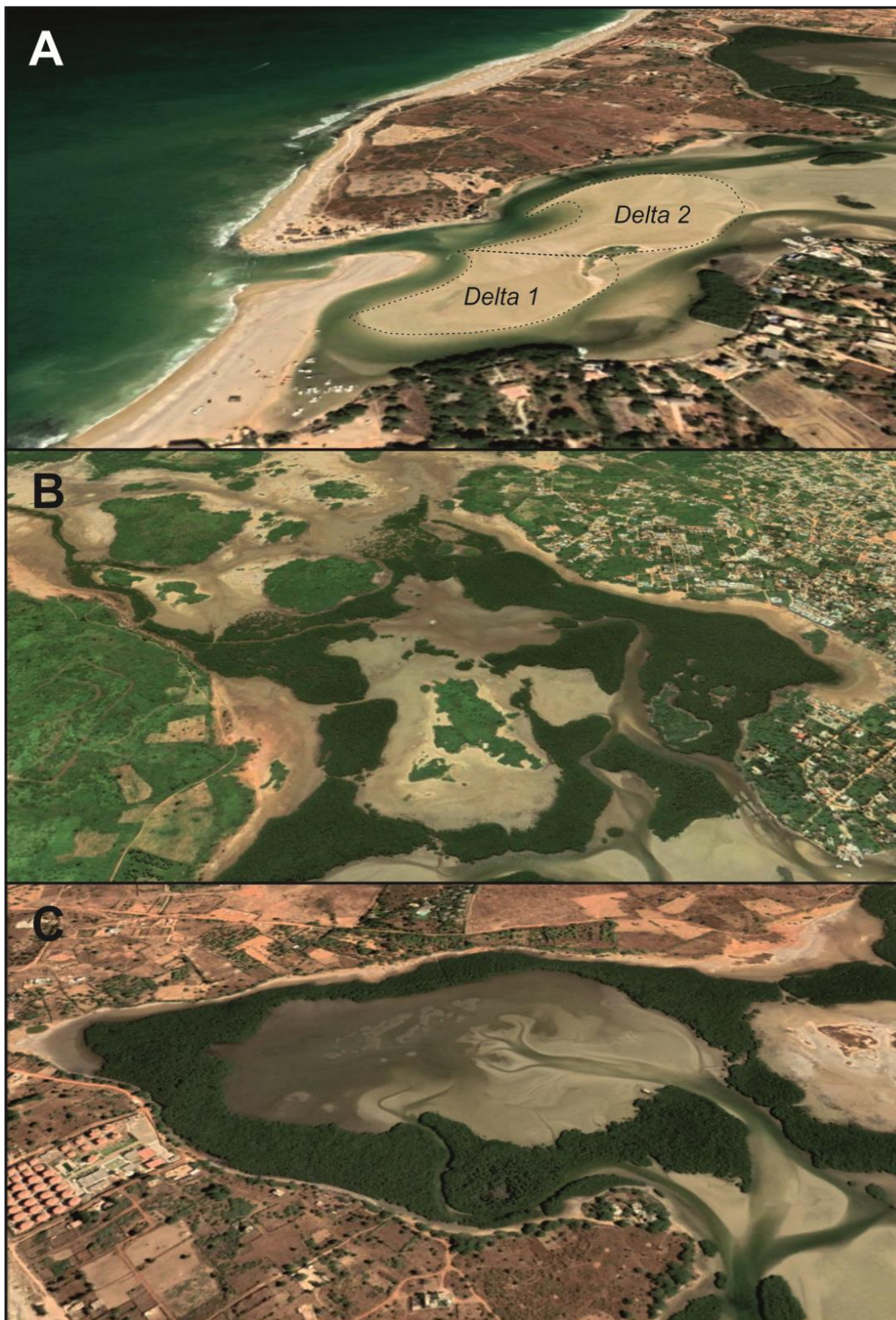


**Figure 2.** Panoramic views of Somone Lagoon. (A) Marine domain displaying spits and flood-tidal deltas. (B) Central basin where tidal flats and mangroves are visible. (C) Guereo Basin where a flood sand delta progrades to the tidal flat facies. Location of panoramic views shown in Figure 1. Images from Google Earth.

### 1.3. Hydrodynamic Setting

The marine domain of this estuary is controlled by South Atlantic waves. There are available wave data measured by using video cameras in the Mbour beach [19], located 14 km to the south (Figure 1). According to these data, locally generated fair-weather-waves are short-crested, with an annual averaged  $H_s$  of 0.5 m and a  $T_p$  of 9.2 s. Seas are directly influenced by the variability of the Intertropical Convergence Zone (ITCZ). The open coast is not affected by locally generated storms, but it is occasionally damaged by external storm swells coming from the deep Atlantic Ocean [20]. These energetic storms are cast by the Southern Annular Mode [21,22]. Statistically, swell storm waves present an annual  $H_s$  average of 1.5 m and  $T_p$  of 3.1 s. Thus, the interannual equatorial climatic fluctuations exert a control on the local variability of wave dimensions and provenances [23,24].

The mean direction provenance of the seas and swell fair-weather waves is from the NW. These constructive waves are the cause of an intense littoral drift which transports an important volume of sands towards the south. There is no information about the magnitude of sand transport in the Small Coast. Along the northern transect of the Senegalese coast, longshore transport was calculated at  $669 \times 10^3 \text{ m}^3/\text{year}$  [20]. However, these data may be not the same in this coastal segment, because the orientation of the coast is different, and the sandy inputs from rivers, such as the Senegal River, are absent. In this case, the longshore transport of sands eroded from cliffs and supplied by small rivers is the main source for the apical growth of the Guereo and Somone Spits, including the tidal deltas developed between them.

The coast where Somone Lagoon is located is micro-tidal with a semidiurnal regime. It presents tides with ranges that oscillate between 1.23 m during mean spring tides and 0.27 m during neap tides, with a mean range of 0.75 m. The tidal prism during spring tides approaches  $3.5 \text{ hm}^3$ , whereas, during neap tides, it is just near  $0.6 \text{ hm}^3$  and during mean tides is  $2.2 \text{ hm}^3$ . The dimensions of average waves and tidal regimes classify this coast as a wave-dominated coast after the criteria established by Davis and Hayes [25].

The Somone River has a highly seasonal regime. Fresh water flow and supplied fluvial sediments are limited to the rainy season (between May and September). The mean annual water contribution for the period 1975–1992 was  $0.49 \text{ hm}^3$ , but it was also a very marked year-on-year irregularity. For the studied period, this annual contribution varies between  $1.43 \text{ hm}^3$  obtained in 1975 and  $0.001 \text{ hm}^3$  in 1992 [26].

Thus, the tidal prism is sensibly greater than the fluvial flow, and most of the time there is a situation of saline inversion due to evapotranspiration in the inner waters of the estuary. The results of Sakho et al. [26] show that, for approximately seven months, from January to July, the estuarine waters are more saline than those entering from the open sea. During this period, it varies from 35 g/L at the mouth to 42 g/L 4 km upstream. During rainy months (from August until November), the fresh waters of Somone River flood into the estuary, and then the gradient becomes normal with a decrease in salinity upstream. Based on the work of these authors, Somone can be described as a dual-functioning estuary from a hydrochemical point of view; it is reverse 70% of the time (from December to July) and normal 30% of the time (August to November).

Mixing processes are also very disrupted by anthropization by means of the building of dams. Water is increasingly retained upstream by multiple hydraulic developments. Two developments are the most controversial, the dam of Idrissa Seck in Nguékhokh and the water reservoir in the Bandia reserve (built for watering animals).

## 2. Materials and Methods

This sedimentological study is based on the information of 14 hand cores distributed on the different domains of the estuary. The cores were obtained by using PVC pipes of 60 mm diameter and maximum length of 1.60 m (Figure 1). The location of the cores was determined by using a Garmin Gecko GPS with an accuracy of one meter. In the laboratory, the PVC pipes were longitudinally cut into two halves with a radial grinder without damage to the sediment. The sediment was also cut using a nylon guitar string.

Once open, the cores were photographed and logged. Lithofacies and sequences were characterized from a detailed description of cores. In each lithofacies, grain size, color, organic content and sedimentary structures (bedding and bioturbation) were characterized.

In each core, several samples were taken at different depths in order to analyze grain size, organic matter and total carbonate content. The depth of each sample in each core was selected according with the different distinguished facies. A total of 61 samples were analyzed.

The grain size of the samples was determined by using a normal Udden–Wentworth sieve column with one phi interval. Normal statistic parameters suggested were determined by the method of Folk and Ward [27], using the software Gradistat 4.0 [24].

For the cores CS-1 and CS-2, which do not contain silt, the sediments collected were first washed with water on a 32  $\mu\text{m}$  sieve to remove salts and impurities and then dried in an oven. Each sample, after drying, was weighed and then decarbonated by cold etching with 30% hydrochloric acid. For the rest of cores, which contained silt, samples were soaked in water with a few drops of  $\text{H}_2\text{O}_2$  and then washed using the 32  $\mu\text{m}$  sieve to retain the maximum before soaking it in HCl. In both cases, after dissolution of the carbonates, the HCl was poured, and the sample was cleanly washed with water, dried and reweighed again. The final weight obtained was subjected to sieving on a series of standard sieves. The weight refusals of the sieves were weighed with a precision balance to the nearest milligram and then recorded on a sieve sheet. The weight of the different sieve rejects had been entered into the Gradistat software, which automatically calculates the weight percentages of each particle size fraction and determines the corresponding particle size parameters. To establish the carbonate content, we measured the weight before and after the decarbonation (g) for each sample.

The total calcium carbonate content was determined by using a Bernard calcimeter from the volume of carbon dioxide released after the sediment sampled was attacked by hydrochloric acid.

Organic content was established based on the dry weight difference between the initial sample and the same sample once digested by hydrogen peroxide 10% vol and desiccated again.

### 3. Results

This study consisted of a detailed description of the lithofacies and lithofacies sequences observed in the cores, including an integrated analysis of grain size, calcium carbonate and organic matter content of the sediment samples along the cores.

#### 3.1. Facies

On the inner estuary, the following four sedimentary sub-environments are present (Figure 1): flood-tidal deltas, tidal flats, mangroves and sabkhas. Each one of them is constituted by characteristic lithofacies sequences, which were studied from the cores and described below.

In the marine domain, flood-tidal deltas occupy the widest area of the estuary mouth (Figure 2A). The facies constituting this environment are represented by the cores CS-1 and CS-2 (Figure 3). These are exclusively sandy facies in which the dominant fractions are medium and fine sand. Grains are mainly composed of quartz, but calcium carbonate grains (small fragments of marine shells) are also abundant. The internal structure mainly consists of metric planar crossbedding sets dipping landwards. On some occasions, like in the base of the core CS-2, the facies are bioturbated by crustacean activity.

In the central domain, wide tidal flats and mangroves are developed (Figure 2B,C). Tidal flats facies are represented in the cores CS-3 to CS-8, so as in the lower part of the core CS-9 (Figures 4 and 5). These cores are constituted by sequences of the following five lithofacies: bioturbated silty sands, bioturbated sandy silts, parallel laminated silts, massive muds and chaotic shell accumulations. All these facies have characteristic dark grey colors related with their high organic matter contents.

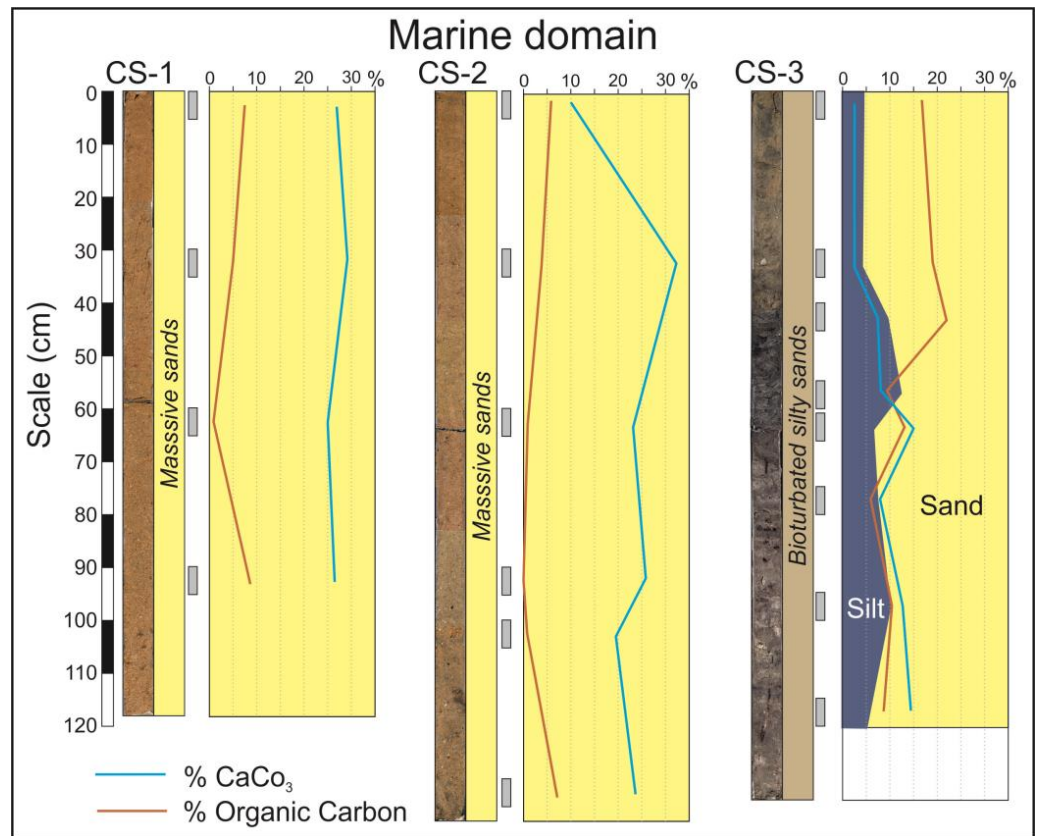


**Figure 3.** Cores from the marine domain of the estuary. The curves indicate the calcium carbonate and organic carbon contents. Blue-yellow surfaces indicate the relative percentage of silt and sand. The gray rectangles indicate the position in the core of the analyzed sediment samples.

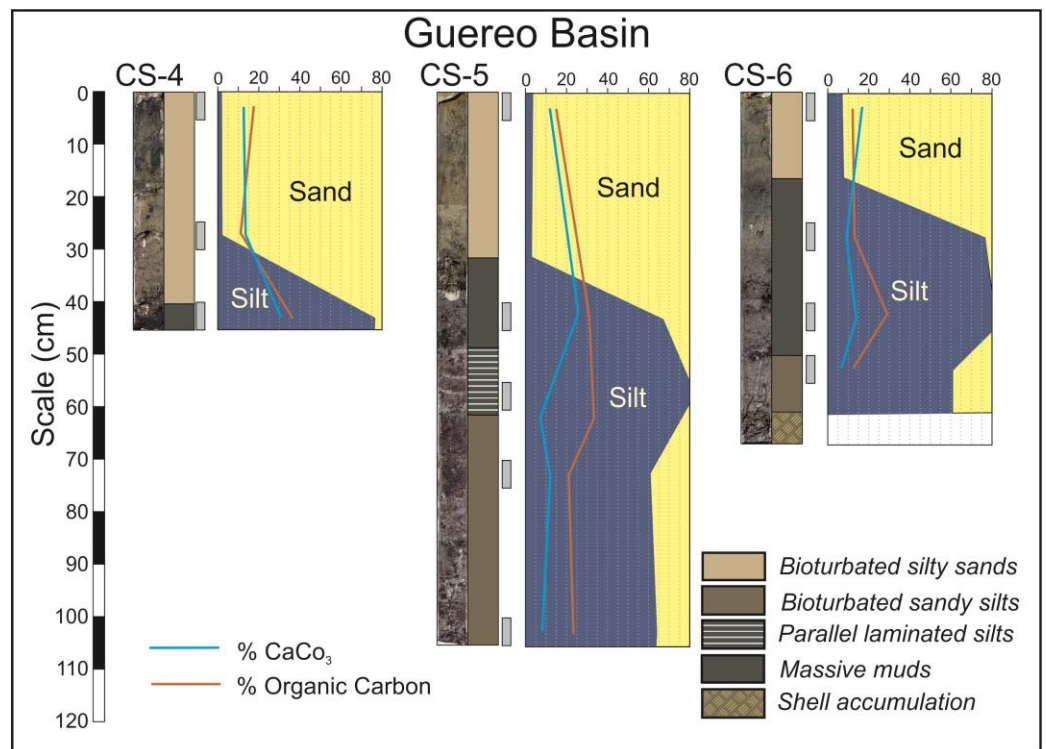


**Figure 4.** Cores from Guereo Basin in the central domain of the estuary.

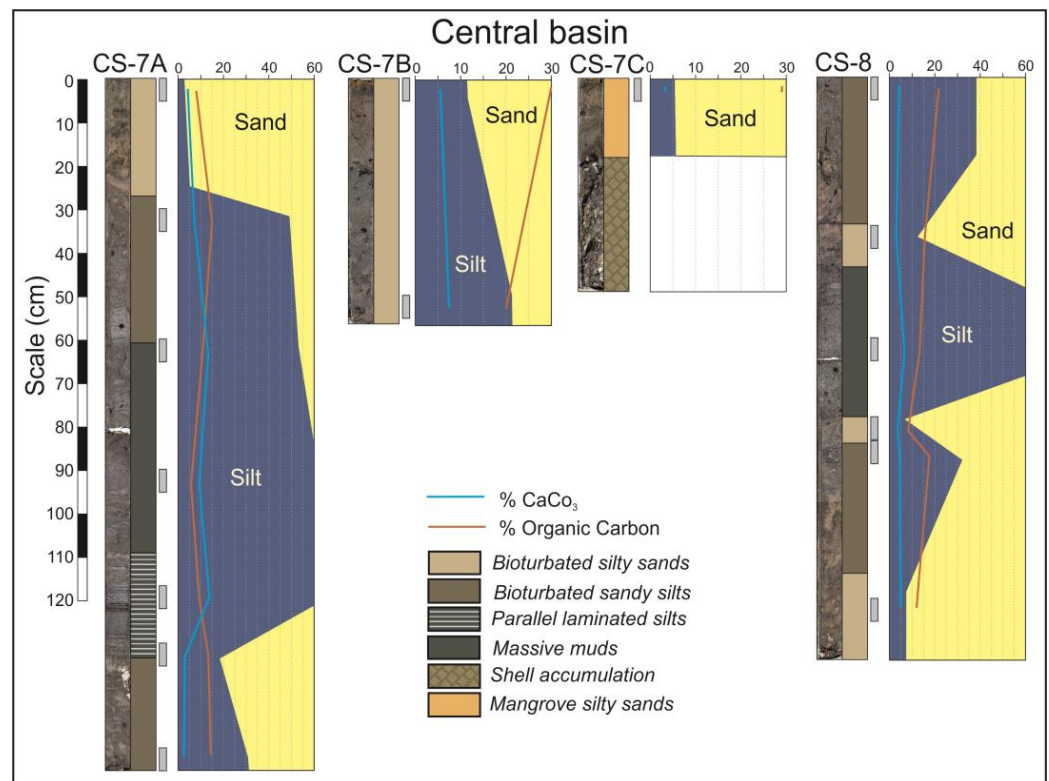


**Figure 5.** Cores from the central basin in the central domain of the estuary.

In the Guereo Basin, the base of cores CS-4, CS-5 and CS-6 (Figure 4) present alternating layers of massive muds, parallel laminated silts, bioturbated sandy silts and shells, but, at the top of the sequences, the only facies present are bioturbated silty sand. This implies that the sediment became sandier in the last stages of infilling.

In the central basin, the inverse case can be observed. The base of the cores CS-7A and CS-8 (Figure 5) is constituted by bioturbated silty sands and becomes finer toward the top. The central part of these cores is constituted by parallel laminated muds, but the degree of bioturbation increases toward the top, which is constituted by massive muds and bioturbated sandy silts. Centimeter layers of shells are occasionally interspersed.

The mangrove facies are observable in the top of the core CS-7C but also in some levels of cores CS-9 and CS-11 that located in the fluvial domain. These facies consist of orangish silty sands and are strongly bioturbated by roots.

Extensive costal sabkhas are developed in the fluvial domain. These sabkhas are the surficial facies of the prograding bay head delta and are observed in the cores CS-9 to CS-12 (Figure 6). The arid climate typical of dry months causes intensive evaporation and a very high salinity that inhibits the presence of vegetation in this environment. The typical facies are an orangish sandy silt which can be massive or horizontally laminated, presenting interspersed salt-rich layers. These facies are usually disposed above the silty tidal flat facies (Figure 6, CS-9) or on sandy fluvial facies (Figure 6, CS-10 and CS-11).

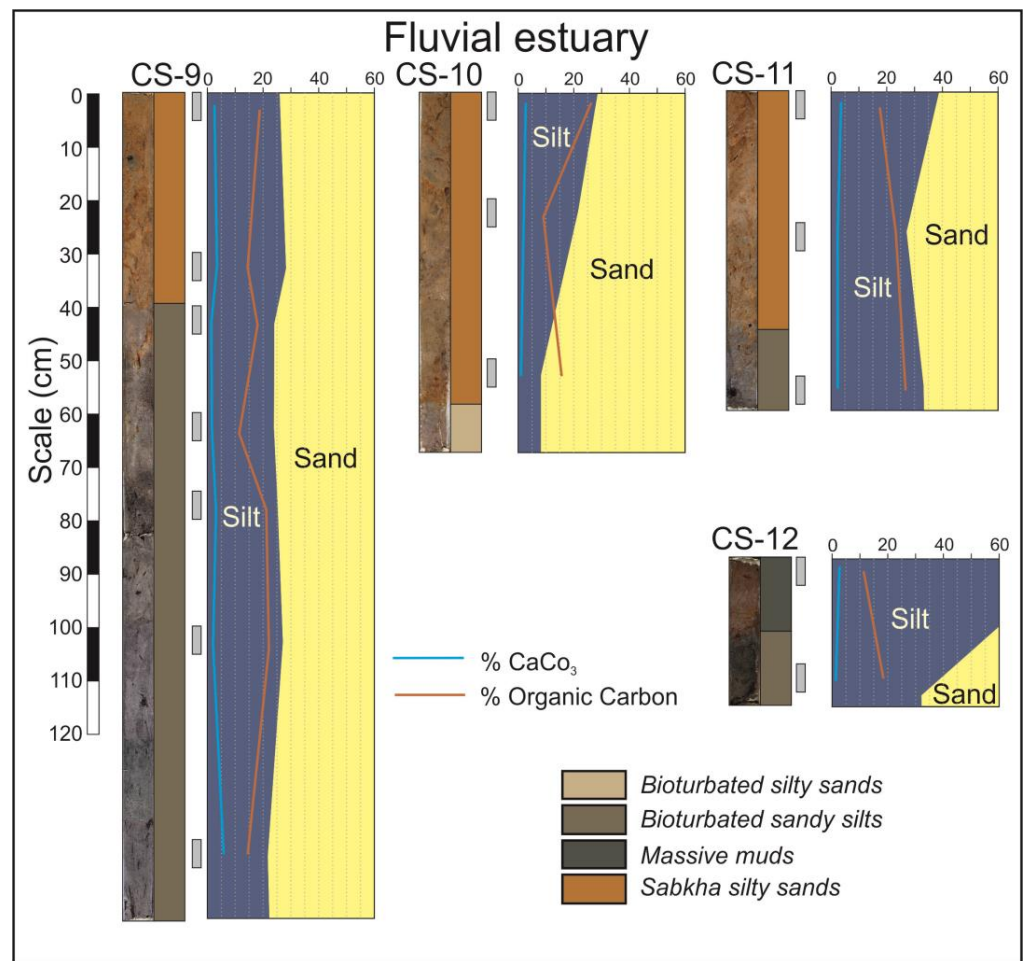


**Figure 6.** Cores from the fluvial domain of the estuary.

### 3.2. Grain Size

The grain size was analyzed in 61 samples, collected at different depths of the cores. The results of these analyses have been represented in cumulative percentage curves. The curves of the same lithofacies are very similar. Thus, the following five groups of grain size types can be distinguished (Figure 7): flood tidal delta sands, tidal flat bioturbated silty sands, tidal flat bioturbated sandy silts, tidal flat massive muds and sabkha sandy silts. From these percentage data, statistic parameters (sorting, kurtosis and skewness) were determined using the software Gradistat [28].

Regarding the sorting (Figure 8A), the flood-tidal delta sand samples are moderately well sorted, whereas tidal flat bioturbated sandy silts and sabkha sandy silts are poorly sorted. Tidal flat bioturbated silty sands present two different types, with the first group being the moderately sorted samples, while the second present a transition from moderately well sorted to well sorted. Tidal flat massive mud samples present a progressive transition from very well sorted to poorly sorted.

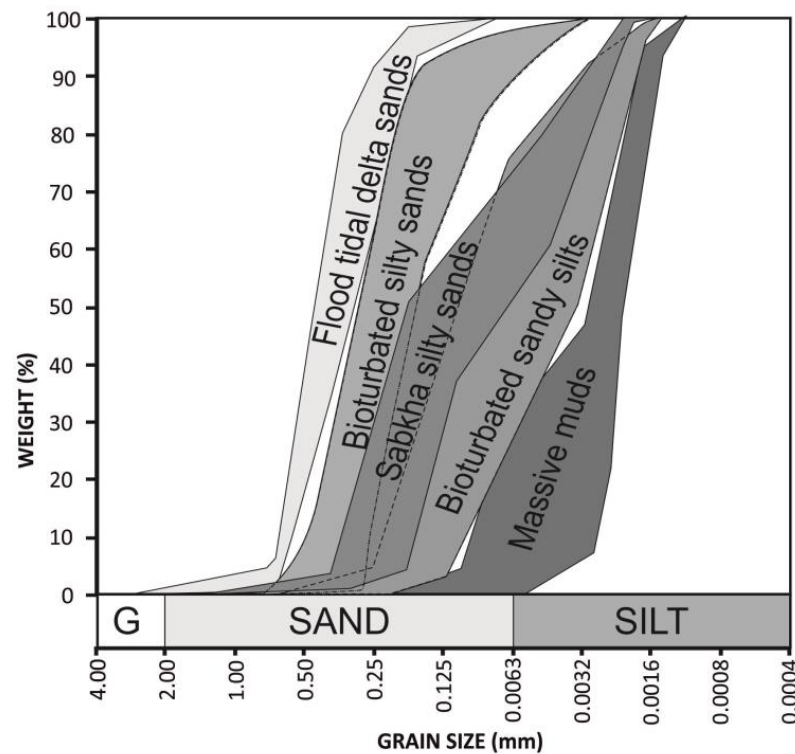


**Figure 7.** Envelopes of grain size cumulated curves of each sub-environment and facies.

Observing the kurtosis (Figure 8B), flood tidal delta sand samples are mainly platykurtic. Bioturbated silty sand samples present a trend line from very leptokurtic to very platykurtic. Bioturbated sandy silt samples are distributed in two clouds of points; the first one is mesokurtic, and the second is very platykurtic. Massive mud samples are also distributed in two-point clouds; the first is very platykurtic, and the other is extremely leptokurtic. Sabkha sandy silt samples are mainly very platykurtic.

Analyzing the skewness, flood tidal delta sands are mainly fine skewed. Bioturbated silty sand and sandy silt samples are mainly very fine skewed, but four samples of silty sands are fine skewed. On the contrary, all the samples of massive muds are very coarse skewed. Sabkha sandy silt samples can be very fine or very coarse skewed.

Based on sorting, kurtosis and skewness do not present a good correlation between them; although, in each lithofacies, there are many samples with common features. In flood tidal delta sands, moderately well-sorted, platykurtic and fine skewed samples dominate, but some samples can also be symmetrical. Bioturbated silty sands are moderately sorted and very fine skewed but divided in two sets according to their kurtosis; the one is very leptokurtic, and the other is mesokurtic. Bioturbated sandy silt samples are poorly sorted, dominating the very platykurtic, very fine skewed samples. Massive muds present two sets of samples. The first one groups well-sorted, extremely leptokurtic and very coarse skewed samples, whereas the second one groups poorly sorted, very platykurtic and very coarse-skewed samples. Sabkha sandy silt samples are poorly sorted, very platykurtic and very fine skewed. Curiously, sabkha samples plot in point clouds that mix them with tidal flat bioturbated sandy silts. Parallel laminated silts and mangrove silts do not present a grain-size distribution distinguishable from tidal flat bioturbated sandy silts or silty sands.

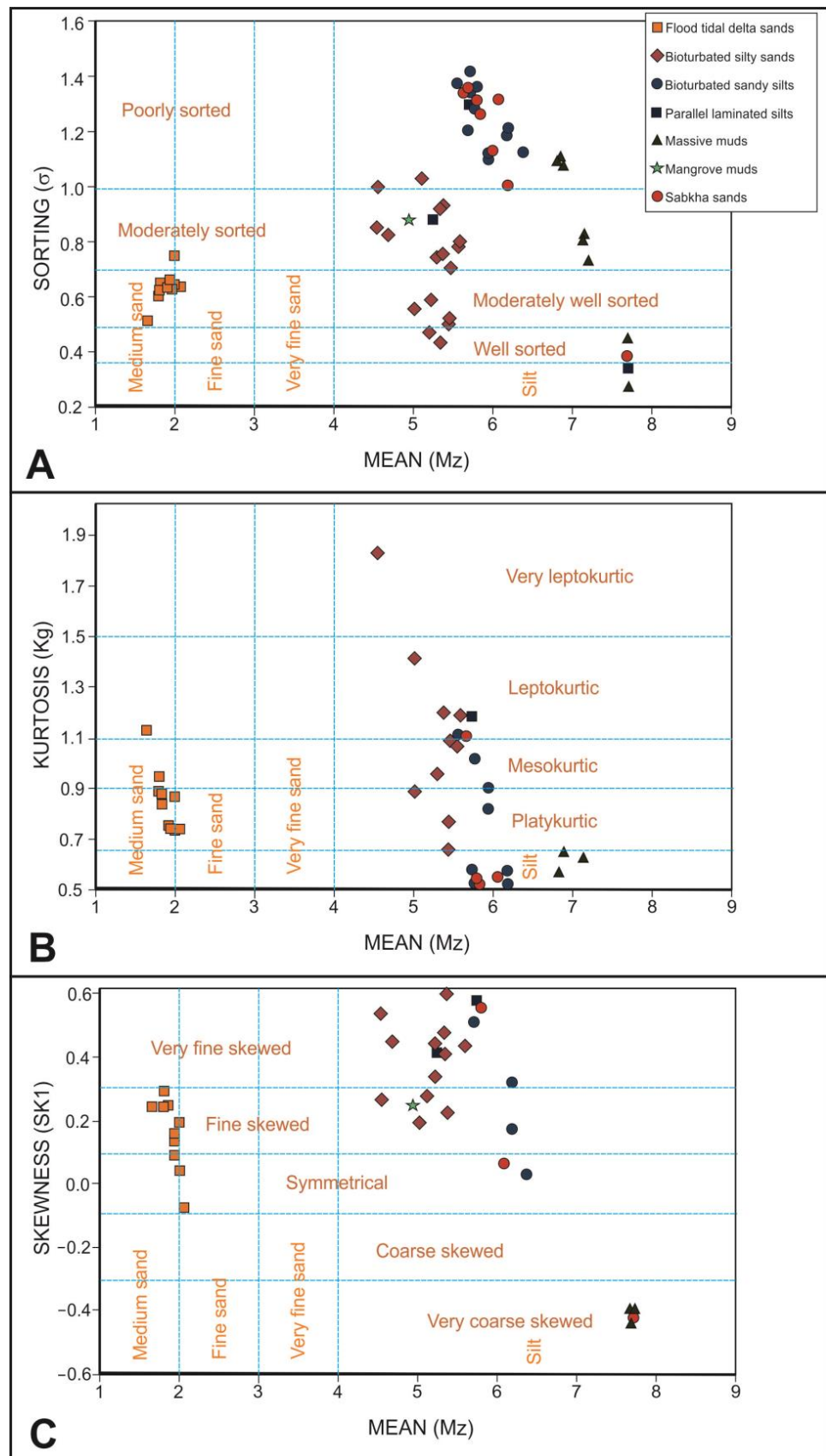


**Figure 8.** Dot diagrams relating the mean grain size with the main studied statistical parameters. (A) Sorting. (B) Kurtosis. (C) Skewness.

### 3.3. Calcium Carbonate Content

The main part of the sediment samples contains a percentage of calcium carbonate less than 15% (Figure 9A). The samples of sabkha silty sands, tidal flat bioturbated sandy silts and bioturbated silty sands present contents even less than 10%. Only the sandy lithofacies from the flood-tidal deltas and some massive muds deposited at depths of 40–45 cm from the surface of the Guereo Basin contain higher percentages, reaching values higher than 25%. The calcium carbonate content is clearly related to the sand content, and two trend lines are observed (Figure 9A). The first one includes the maximum contents in the flood tidal delta sands and diminished to the Guereo Basin silty sands to present the minimum contents of the central basin silty sands. The second trend line start in the massive muds of the central basin, through the bioturbated sandy silts of the tidal flats in the same central basin to finish in the minimum values of the sabkha sandy silts.

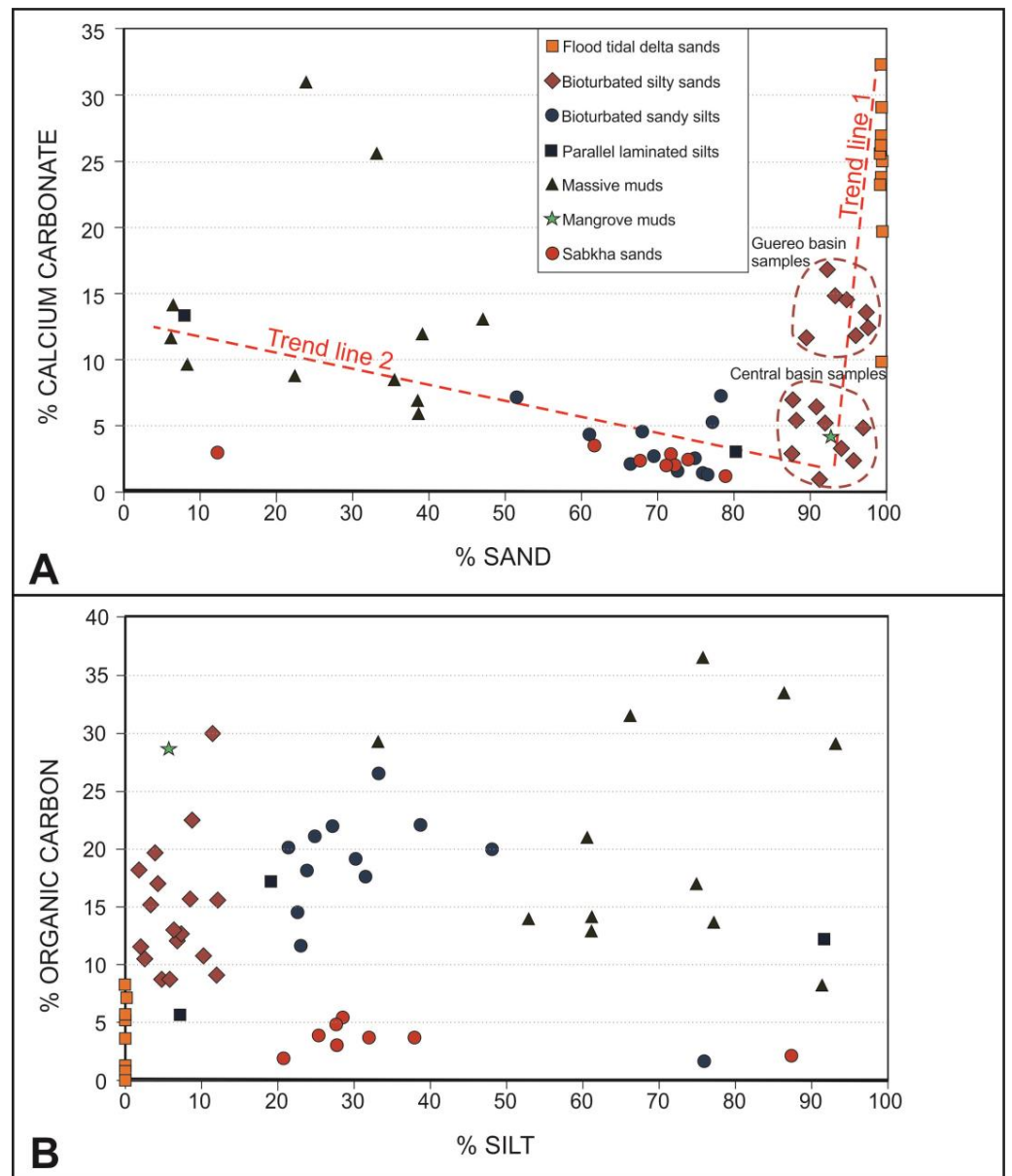


**Figure 9.** Dot diagrams relating the sand and silt contents with the calcium carbonates (A) and organic carbon (B).

### 3.4. Organic Matter

The organic matter content is unevenly distributed (Figure 9B). In general, facies that present dark gray tones are those that have a higher content of organic matter. In this way, the facies with a lower organic content are those present in the flood-tidal deltas and those of the sabkhas developed in the fluvial domain of the estuary. The main part of the samples of these environments presents contents less than 5%. The organic content of the rest of the facies varies between 10 and 35%, without there being a direct relationship with the fine-sized sediment fractions or inverse with the carbonates, as occurs in other estuaries.

## 4. Discussion

In general terms, there is a clear pre-eminence of sands in all the domains and sub-environments of this estuary. The outer facies present high percentages of medium and fine sands transported as bedload, and this sand content decreases to the tidal flat facies of the central basin and Guereo Basin at the same time that the percentage of the silts increase. In these areas, the dominant sand fractions are fine and very fine sands. The maximum percentage of silts is reached just in the tidal flats where cores CS-7A, B and C are located. The dominance of silts in the central basin demonstrates the importance of the tidal slacks on the deposition process in this sector of the estuary. From this area, the sand content grows again in the direction of the fluvial domain. This sediment distribution showing a clear textural bipolarity is typical in all wave-dominated estuaries (e.g., [10,29] among many others). Nevertheless, in most documented cases, the predominance of fine material in the central domain of the estuary was considered as a result of the mixture between decantation of suspended matter from fluvial origin and physical–chemical processes (flocculation) related with the water wedge [29]. In the Somone Lagoon, the main part of the fine matrix is silt. Then the mechanical processes seem to be more important than those induced by the mingling of waters, so the deposition of fine material could be attributed to decantation and not to flocculation.

A notable characteristic of these estuarine facies is their high degree of bioturbation. Crustaceans, annelids, mollusks, fishes and birds stir up surface sediment on tidal flats, and the roots of *Rhizophora mangle*, *Rhizophora racemosa* and *Avicennia africana* bioturbate the mangrove sediments. On very few occasions, non-bioturbated facies have been seen. Thus, parallel laminated silts facies only appear in short sections of cores CS-3, CS-5 and CS-7A. Bioturbation is not visible in massive muds, because there is not lithological contrast, but these facies are also bioturbated. This high bioturbation is indicative of the high activity of all organisms of the food chain in the estuary due to the tranquility of the environment and the low energy of the tidal currents [30]. Macrobenthos activity on the estuarine bed contributes to increases in the sediment–air surface of contact during low tides, influencing the redox conditions, oxidizing the organic matter and affecting chemical cycles [31–33].

Although intensive bioturbation processes favor the oxidation of organic matter, the organic carbon content is quite high in the estuarine tidal flat sediments. The organic carbon in estuaries is normally attributed to flocculation processes associated with the mix of fresh and salt waters [29,34]. However, as it was previously analyzed, the dominant silty grain size suggests that flocculation processes are of little importance in this estuary. On the contrary, in this case, the organic carbon accumulation in the estuarine facies appears to be higher than the capacity of the bioturbation to oxidize it. In fact, the biological activity of this estuary may be in fact the origin of much of the organic matter preserved in the sediments. It has been cited that pelletal [35], algal [36] or fulvic/humic acids [37] can be the origin of autochthonous organic carbon in estuaries. In the case of tropical systems with a deficient tidal drainage, these receive an important nutrient supply from the fluvial source during wet spring periods [38]. Discriminating between these possible sources would require further works about carbon isotopic identification.

In addition, wave-dominated microtidal estuaries have high nutrient-retention efficiency, because nutrients remain in the central basin due to the inability of tides to rework the sediments to open areas [38]. The small tidal prism of this estuary and the narrow

inlet of the marine domain suggest that a lack of tidal drainage contributes to retain and preserve the carbon in the sediments.

Finally, another influence on the sediment composition is the chemical and biochemical productivity of calcium carbonate. On one hand, a part of the calcite has a biological marine origin due to an upwelling process on this coast and come into the estuary from the open sea [39]. This circumstance results in a large number of mollusks, whose shells are fragmented and reworked by waves when they die and are introduced into the estuary by the tides. On the other hand, the evaporitic processes occurring in tidal flats located on the inner areas of tropical estuaries also usually generate a precipitation of aragonite, calcite and dolomite [40,41]. In this case, the clear decrease in carbonate contents from the marine domain to the inner areas is clearly related with the sand content of the sediment. That demonstrates that the main part of the calcium carbonate is introduced in the estuary from the sea by flood tidal currents. Only the massive mud facies of the central sector of the estuary, especially in the Guereo Basin, have a significant calcium carbonate content that can be attributed to evaporitic processes. These evaporitic processes have been highlighted in this estuary by some authors who have observed an inversion of salinity during the dry months in which the river does not introduce freshwater flow into the estuary [26]. There is a typical duality occurring commonly in small estuaries in tropical areas of the southern hemisphere, which can vary from freshwater-dominated systems during periods of fluvial floods to completely tide-dominated systems during dry periods [42,43]. In this case, a deficient tidal drainage related with the microtidal character of the estuary, and the high degree of clogging, favors this domain of evaporation during dry periods when the massive muds are deposited, while during wet periods the river floods introduce the main part of the suspended fine sands and silts that characterize the inner facies of the estuary.

The vertical variability in the facies sequence of the cores tells us about the evolution in the sedimentation conditions of the estuary. In the case of the central basin, it is observed that the sediment becomes finer towards the top of the sequence. This indicates that the infilling of the estuary has produced a relative disconnection of the central sector of the estuary from the sources of marine and river sand. However, the cores of the Guereo Basin show that, towards the top, the facies become sandy again. This is related to the entry into the system of sand from the marine source introduced by the tides. This is facilitated by the increasing degree of channelization related to the development of the second flood tidal delta. The sandy delta formed in the Guereo Basin with slit sands from the marine domain is visible in aerial views (Figure 2C).

In the fluvial domain of the estuary, the sediments of the bay head delta covered previous tidal flat facies until reaching the supratidal zone and developing an extensive sabkha. However, it is striking that the mineral content related to evaporation (like calcium carbonate) is not very abundant in its facies. This can be attributed to the fact that the sabkha is only the superficial expression of the bay head delta. Thus, the facies present in the cores are not all properly evaporitic but facies characteristic of the delta progradation from fluvial sediments are. The presence of root bioturbation in the lower facies of the sequence can be identified with the presence of previous mangroves in these areas whose plants would be eliminated by the overexposure and hypersalinity typical of the supratidal evaporitic environment. Then the evaporation process only occurs at the final critical stage and is just preserved in the last millimeters of the core. Nevertheless, it may be that other evaporitic minerals such as sulfates or halides are present in the sediment; in future campaigns, these minerals should be analyzed.

## 5. Conclusions

The Somone Lagoon is an example of a microtidal, wave-dominated tropical estuary with elevated evaporation rates. This set of characteristics makes this estuary a natural laboratory to analyze the influence of individual and linked processes on the generation and preservation of facies, which differs from other well-studied, wave-dominated estuaries (mesotidal and warm-climate). From a morphosedimentary point of view, this system

has the characteristics of a wave-dominated estuary in an advanced state of infilling. The distinctive division into domains of this type of estuary is clearly visible. The high degree of infilling is evidenced in the presence of wide tidal flats in the central domain of the estuary, including mangroves and sabkhas in the fluvial domain. In the marine domain, the advanced stage of clogging is manifested in the development of two successive flood-tidal deltas, prograding to the inner estuary. Carbonate sands are introduced by tidal flood currents and distributed from the tidal flood deltas to the inner areas of the estuary.

The tropical character of the estuary is manifested in several morphological and dynamic aspects, especially in the fact that mangroves replace the salt marshes typical of mid-latitude estuaries. The existence of two marked seasons conditions the dynamics of the estuary. During the rainy season, the river introduces large amounts of fine sand, silt and nutrients into the system, which are distributed towards the central domain of the estuary. During the dry season, the evaporation is the dominant process. During this period, the salinity of the estuary is higher than that of seawaters. It is then that large areas of sabkhas develop in supratidal zones, especially in the fluvial domain, on top of the bay head delta sequence.

The microtidal character of the estuary is shown in poor drainage that favors the trapping of organic matter inside the estuary. This organic matter is the basis of the richness of the food chain, manifested in the abundance of bioturbation in estuarine facies.

The sedimentary sequence observed in the cores shows a progressive filling of the estuary, which manifests in a fining-upwards facies sequence. However, the increased degree of channelization means that currents can, through these tidal channels, transport sand more easily towards the center of the estuary from both marine and river sources. For this reason, the Guereo Basin cores show that the grain size increases again towards the top of the sequence.

**Author Contributions:** Conceptualization, C.I.Y. and J.A.M.; methodology, J.A.M.; software, A.G. and M.F.D.; validation, I.-S.S. and E.S.; formal analysis, E.G.-V.; investigation, J.A.M.; resources, C.I.Y.; data curation, A.G.; writing—original draft preparation, J.A.M.; writing—review and editing, E.G.-V.; visualization, J.A.M.; supervision, E.S.; project administration, C.I.Y.; funding acquisition, C.I.Y. All authors have read and agreed to the published version of the manuscript.

**Funding:** This research was funded by the Direction of Geology of the Ministry of Mines and Geology. Republic of Senegal, Project: Inventory, Evaluation and valorization of geosites throughout the territory of Senegal. Project number C\_P2-MMG\_059.

**Institutional Review Board Statement:** The study did not require ethical approval.

**Informed Consent Statement:** Not applicable.

**Data Availability Statement:** Data unavailable due to privacy.

**Acknowledgments:** The authors would like to acknowledge the people working at the office of International Relationships of the University of Huelva, who facilitated all the administrative processes to travel to Senegal during the field survey, as well as the Department of Geology of the Cheikh Anta Diop University for their support during the field and laboratory works. We also acknowledge the comments and suggestions provided by two anonymous reviewers, which substantially contributed to the improvement of the manuscript.

**Conflicts of Interest:** The authors declare no conflicts of interest. The funders had no role in the design of the study; in the collection, analyses, or interpretation of data; in the writing of the manuscript or in the decision to publish the results.

## References

1. Pritchard, D.W. What is an estuary? Physical viewpoint. In *Estuaries*; Lauff, G.H., Ed.; American Association for the Advancement of Science Publication: Washington, DC, USA, 1967; Volume 83, pp. 3–5.
2. Morales, J.A. *Coastal Geology*; Springer Nature: Berlin/Heidelberg, Germany, 2022; 455p.
3. Russell, R.J. Origin of estuaries. In *Estuaries*; Lauff, G.H., Ed.; American Association for the Advance of Science Publication: Washington, DC, USA, 1967; Volume 83, pp. 93–99.

4. McManus, J. Temporal and spatial variations in estuarine sedimentation. *Estuaries* **1998**, *21*, 622–634. [[CrossRef](#)]
5. Pritchard, D.W. Estuarine circulation patterns. *Proc. Am. Soc. Civ. Eng.* **1955**, *81*, 717/1–717/11.
6. Pritchard, D.W. Salt balance and exchange rate for Chincoteague Bay. *Chesap. Sci.* **1960**, *1*, 48–57. [[CrossRef](#)]
7. Le Floch, J. Propagation of the Tide in the Seine Estuary and Seine-Maritime. Ph.D. Thesis, University of Paris, Paris, France, 1961; 507p. (In French)
8. Hayes, M.O. Morphology of sand accumulation in estuaries: An introduction to the symposium. In *Estuarine Research*; Cronin, L.E., Ed.; Academic Press: New York, NY, USA, 1975; Volume 2, pp. 3–22.
9. Fairbridge, R.W. The estuary: Its definition and geodynamic cycle. In *Chemistry and Biogeochemistry of Estuaries*; Olausson, E., Cato, I., Eds.; John Wiley and Sons: New York, NY, USA, 1980; pp. 1–36.
10. Dalrymple, R.W.; Zaitlin, B.A.; Boyd, R. Estuarine facies models: Conceptual basis and stratigraphic implications. *J. Sediment. Petrol.* **1992**, *62*, 1130–1146. [[CrossRef](#)]
11. Anthony, E.J.; Oyede, L.M.; Lang, J. Sedimentation in a fluvially infilling, barrier-bound estuary on a wave-dominated, microtidal coast: The Ouémé River estuary, Benin, West Africa. *Sedimentology* **2002**, *49*, 1095–1112. [[CrossRef](#)]
12. Flor-Blanco, G.; Flor, G.; Morales, J.A.; Pando, L. Hydrodynamic controls of morpho-sedimentary evolution in a rockbounded mesotidal estuary. Tina Menor (N Spain). *J. Iber. Geol.* **2015**, *41*, 315–332.
13. Plint, A.G.; James, N.P.; Dalrymple, R.W. Wave- and storm-dominated shoreline and shallow-marine systems. In *Facies Models 4*; James, N.P., Dalrymple, R.W., Eds.; Geological Association of Canada: St. John, NL, Canada, 2010; pp. 167–199.
14. Yoon, H.H.; Lee, J.Y.; Kim, J.C.; Jun, C.P.; Choi, H.W. Incised-valley filling sedimentation in a small river valley of a wave-dominated, embayed coast in response to Holocene sea level rise, Yeongil Bay, Southeastern Korea. *Mar. Geol.* **2023**, *464*, 107127. [[CrossRef](#)]
15. Roger, J.; Banton, O.; Barousseau, J.P.; Castaigne, P.; Comte, J.-C.; Duvail, C.; Nehlig, P.; Noël, B.J.; Serrano, O.; Travi, Y. *Explanatory Note for Multi-Layer Mapping at 1/50,000 and 1/20,000 of the Cape Green Activity Area*; Direction of Mines and Geology; Ministry of Mines, Industries and PME of Senegal: Dakar, Senegal, 2009; 245p. (In French)
16. Michel, P. The southwestern Sahara margin: Sediments and climate change during the recent Quaternary. *Palaeoecol. Afr. Surround. Isl.* **1980**, *12*, 297–306.
17. Giresse, P.; Barousseau, J.-P.; Causse, C.; Diouf, B. Successions of sea-level changes during the Pleistocene in Mauritania and Senegal distinguished by sedimentary facies study and U/Th dating. *Mar. Geol.* **2000**, *170*, 123–139. [[CrossRef](#)]
18. Kaly, J.L.; Sy, B.A.; Dia, I.; Bodian, A.; Sy, A.A.; Mbou, O.; Faye, C.A.T. *Bathymetric Study of the Somone Lagoon*; Environmental Report 2015; Ministry of Environment and Sustainable Development of Senegal: Dakar, Senegal, 2015; 123p. (In French)
19. Abessolo-Ondoa, G.; Almar, R.; Kestenare, E.; Bahini, A.; Houngue, G.H.; Jouanno, J.; Du Penhoat, Y.; Castelle, B.; Melet, A.; Meyssignac, B.; et al. Potential of video cameras in assessing event and seasonal coastline behaviour: Grand Popo, Benin (Gulf of Guinea). *J. Coast. Res.* **2016**, *75*, 442–446. [[CrossRef](#)]
20. Sadio, M.; Anthony, E.; Diaw, A.; Dussouillez, P.; Fleury, J.; Kane, A.; Almar, R.; Kestenare, E. Shoreline Changes on the Wave-Influenced Senegal River Delta, West Africa: The Roles of Natural Processes and Human Interventions. *Water* **2017**, *9*, 357. [[CrossRef](#)]
21. Almar, R.; Kestenare, E.; Reyns, J.; Jouanno, J.; Anthony, E.J.; Laibi, R.; Hemer, M.; Du Penhoat, Y.; Ranasinghe, R. Response of the Bight of Benin (Gulf of Guinea, West Africa) coastline to anthropogenic and natural forcing, Part1: Wave climate variability and impacts on the longshore sediment transport. *Cont. Shelf Res.* **2015**, *110*, 48–59. [[CrossRef](#)]
22. Laibi, R.; Anthony, E.; Almar, R.; Castelle, B.; Senechal, N.; Kestenare, E. Longshore drift cell development on the human-impacted Bight of Benin sand barrier coast, West Africa. *J. Coast. Res.* **2014**, *70*, 78–83. [[CrossRef](#)]
23. Diallo, M.A.; Keita, I.N. The ocean data information in Senegal. The ocean data and information network in Africa. Report of the project ODINAFRICA-III. UNESCO, 2009. pp. 133–138. Available online: <https://unesdoc.unesco.org/ark:/48223/pf0000186903> (accessed on 9 January 2024).
24. Wade, M.; Mignot, J.; Lazar, A.; Gaye, A.T.; Carré, M. On the spatial coherence of rainfall over the Saloum delta (Senegal) from seasonal to decadal time scales. *Front. Earth Sci.-Atmos. Sci.* **2015**, *3*, 30. [[CrossRef](#)]
25. Davis, R.A.; Hayes, M.O. What is a wave-dominated coast? *Mar. Geol.* **1984**, *60*, 313–329. [[CrossRef](#)]
26. Sakho, I.; Mesnage, V.; Deloffre, J.; Lafite, R.; Niang, I.; Faye, G. Role of climate forcing and anthropogenic pressure on tropical mangrove ecosystems: The Somone case (Senegal). *Pangea Spec. Vol.* **2010**, *47/48*, 69–75.
27. Folk, R.L.; Ward, W.C. Brazos River bar: A study in the significance of grain size parameters. *J. Sediment. Petrol.* **1957**, *27*, 3–26. [[CrossRef](#)]
28. Blott, S. *Graidstat 4.0*; A Grain-Size Distribution and Statistics Package for the Analysis of Unconsolidated Sediments by Sieving or Laser Granulometer; Free Distribution Software; Surface Processes and Modern Environments Research Group, University of London: London, UK, 2000.
29. Dyer, K.R. Sediment processes in estuaries: Future research requirements. *J. Geophys. Res.* **1989**, *97*, 14327–14339. [[CrossRef](#)]
30. Swinbanks, D.D.; Murray, J.W. Biosedimentological zonation of boundary bay tidal flat, Fraser river delta, British Columbia. *Sedimentology* **1981**, *28*, 201–237. [[CrossRef](#)]
31. Kristensen, E.; Alongi, D.M. Control by fiddler crabs (*Uca vocans*) and plant roots (*Avicennia marina*) on carbon, iron and sulfur biogeochemistry in mangrove sediment. *Limnol. Oceanogr.* **2006**, *51*, 1557–1571. [[CrossRef](#)]

32. Xiao, K.; Pan, F.; Santos, I.R.; Zheng, Y.; Zheng, C.; Chen, N.; Lu, Z.; Wang, F.; Li, Z.; Li, H. Crab bioturbation drives coupled iron-phosphate-sulfide cycling in mangrove and salt marsh soils. *Geoderma* **2022**, *424*, 115990. [[CrossRef](#)]
33. Pan, F.; Xiao, K.; Cai, Y.; Li, H.; Guo, Z.; Wang, X.; Zheng, Y.; Zheng, C.; Bostick, B.C.; Michael, H.A. Integrated effects of bioturbation, warming and sea-level rise on mobility of sulfide and metalloids in sediment porewater of mangrove wetlands. *Water Res.* **2023**, *233*, 119788. [[CrossRef](#)] [[PubMed](#)]
34. Kimeli, A.; Cherono, S.; Mutisya, B.; Tamooh, F.; Okello, J.; Westphal, H.; Koedam, N.; Kairo, J. Tracing organic matter sources in the estuarine sediments of Vanga, Kenya, and provenance implications. *Estuar. Coast. Shelf Sci.* **2021**, *263*, 107636. [[CrossRef](#)]
35. Guo, S.; Sun, J.; Wang, Y. Production and export of copepods fecal pellets in an eutrophic coastal sea: The Changjiang (Yangtze River) estuary. *Estuar. Coast. Shelf Sci.* **2019**, *218*, 163–172. [[CrossRef](#)]
36. Kang, P.; Zhang, H.; Yang, Z.; Zhu, Y.; He, B.; Li, Q.; Lee, C.; Tang, T. A model of algal organic carbon distributions in the Pearl River estuary using the amino acid carbon isotope values. *Geochim. Cosmochim. Acta* **2021**, *294*, 1–12. [[CrossRef](#)]
37. Sarma, N.S.; Chiranjeevulu, G.; Pandi, S.R.; Rao, D.B.; Sarma, V.V.S.S. Coupling between chromophoric dissolved organic matter and dissolved inorganic carbon in Indian estuaries. *Sci. Total Environ.* **2023**, *905*, 167120. [[CrossRef](#)] [[PubMed](#)]
38. Gao, Y.; Jia, J.; Lu, Y.; Sun, K.; Wang, J.; Wang, S. Carbon transportation, transformation, and sedimentation processes at the land-river-estuary continuum. *Fundam. Res.* **2022**, *in press*. [[CrossRef](#)]
39. Weldeab, S.; Lea, D.W.; Schneider, R.R.; Andersen, N. 155,000 years of West African monsoon and ocean thermal evolution. *Science* **2007**, *316*, 1303–1307. [[CrossRef](#)] [[PubMed](#)]
40. Shinn, E. Tidal flat environment. In *Carbonate Depositional Environments*; Scholle, P.A., Bebout, D.G., Moore, C.H., Eds.; Memoir 33; American Association of Petroleum Geologists: Tulsa, OK, USA, 1983; pp. 171–210.
41. Gavish, E. Recent sabkhas marginal to the southern coast of Sinai, Red Sea. In *Hypersaline Brines and Evaporitic Environments*; Nissenbaum, A., Ed.; Developments in Sedimentology, 28; Elsevier: Amsterdam, The Netherlands, 1980; pp. 233–251.
42. Eyre, B. Regional evaluation of nutrient transformation and phytoplankton growth in nine river-dominated subtropical east Australian estuaries. *Mar. Ecol. Prog. Ser.* **2000**, *205*, 61–83. [[CrossRef](#)]
43. Taljaard, S.; van Niekerk, L.; Joubert, W. Extension of a qualitative model on nutrient cycling and transformation to include microtidal estuaries on wave-dominated coasts: Southern hemisphere perspective. *Estuar. Coast. Shelf Sci.* **2009**, *85*, 407–421. [[CrossRef](#)]

**Disclaimer/Publisher's Note:** The statements, opinions and data contained in all publications are solely those of the individual author(s) and contributor(s) and not of MDPI and/or the editor(s). MDPI and/or the editor(s) disclaim responsibility for any injury to people or property resulting from any ideas, methods, instructions or products referred to in the content.